

Entrainment and spreading of turbulent shear flows

Jimmy Philip, Kapil Chauhan and Ivan Marusic

Department of Mechanical Engineering
 The University of Melbourne, Victoria, 3010 AUSTRALIA

Abstract

Over the last decade there has been a renewed interest in understanding the entrainment process in turbulent shear flows [5]. Even though there are differences between the way different shear flows (such as jets, wakes, boundary layers and shear-free flows) develop [14], the origin of these differences is not clear. Here, employing experimental data from an axisymmetric turbulent jet and a turbulent boundary layer, we present conditional velocity profiles at the turbulent/non-turbulent interface (TNTI) and quantitatively reveal the differences encountered by the two different shear flows. In particular, we examine the role of radial velocity in the entrainment process which is present in jets and is absent for boundary layers (and wake flows). We consider the turbulent kinetic energy budget for the axisymmetric jet to illustrate the dominant role of ‘radial advection’ compared to ‘streamwise advection’, clarifying the important role of the radial velocity at the interface in jet entrainment which is absent in boundary layers. Subsequently, we classify the shear-flows for entrainment based on the large- and small-scale mechanisms. Finally, a simplified approach by which the scaling of ‘small scale’ entrainment velocity can be used to derive the well known overall ‘large scale’ spreading of turbulent shear flows is presented.

Introduction and objectives

Research in the area of entrainment has undergone a dramatic increase over the past few years [5], primarily fuelled by large scale computations (e.g., [6, 19]) and particle image velocimetry (PIV) measurements (e.g., [20, 2, 15, 3]). The turbulent/non-turbulent interface (TNTI) is suggested to be dominated by small-scale, viscous, diffusive activity called ‘nibbling’ [20], where nibbling is the mechanism by which ‘non-turbulent fluid’ is converted into ‘turbulent fluid’ [5]. Classically, however, entrainment has been attributed to large-scale mechanisms collectively referred to here as ‘engulfment’ [18]. The main reason for considering large-scales is that the evolution of different canonical flows such as turbulent jets, wakes and boundary layers are different and this evolution can be described by the large-scale mean properties of the flow. Furthermore, these turbulent flows have been observed to be dominated by large-scale coherent structures. A small-scale-only mechanism would suggest a development that is similar for different shear flows which is contrary to the observations. To reconcile this, Philip *et al* [14] suggested a ‘multi-stage’ entrainment process which is different for different shear flows, in which the initial stages are large-scale dominated and the final stage is always nibbling. Another way to accommodate the large- and small-scale process is by considering entrainment as a ‘multi-scale’ phenomenon, which can be evidenced by filtering the equations of motion at different length scales (where engulfment is defined with largest and nibbling by the smallest filter size, respectively) [15]. A fractal TNTI surface (e.g., [7]) following [16] and [13] would be consistent with such a multi-scale approach.

As such, the first two objectives of this paper are: (i) to characterise differences between jets and boundary layer flows concerning entrainment across TNTI, thus testing the validity of the

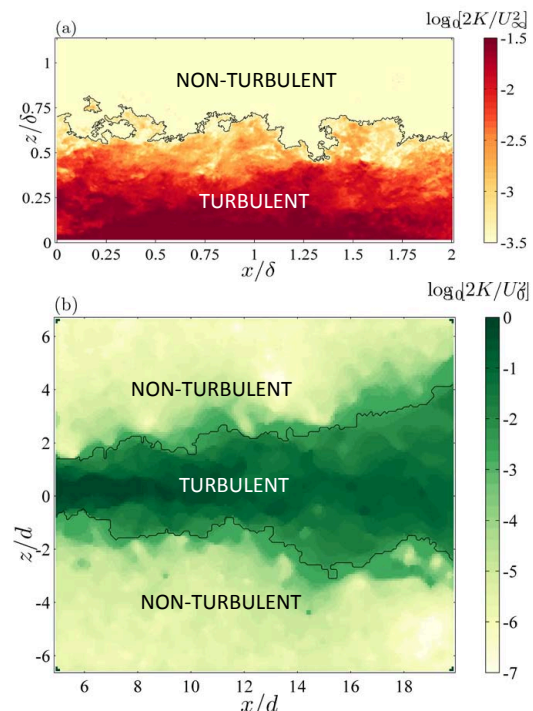


Figure 1: Kinetic Energy contours demarcating the turbulent from the non-turbulent regions. (a) A boundary layer flow from left to right at $Re_\tau = 14500$. (b) Jet flow from left to right, at $Re_d = 3000$.

‘multi-stage’ entrainment process [14]; and, (ii) extend the classification of shear flows for entrainment studies by Philip *et al* [14] into various large and small scale contributions.

Another interesting fact that has emerged from the recent studies on TNTI is the scaling of velocities at TNTI. It has been shown that the ‘entrainment velocity’ (velocity of the fluid relative to the velocity of TNTI) scales with the local fluctuating fluid velocities in shear-free flows and boundary layers [9, 15, 3]. This suggests that the overall entrainment or the consequent growth/spreading of the various flows could somehow be calculated from the scaling of the ‘local’ entrainment velocity. Classically, however, the growth/spreading are only predicted from the mean quantities. Therefore, our final objective, (iii) is to provide a simple derivation starting from the scaling of ‘local’ entrainment velocities leading to the overall growth/spreading rates.

Comparing TNTI properties of boundary layers and jets

For the TNTI analysis we employ the following experimental databases. The turbulent boundary layer database is the same as that used by [7, 2, 3] and [15]. An example is shown in figure 1(a) where the flow is from left to right, at friction Reynolds number $Re_\tau = u_\tau \delta / \nu = 14500$. Here, the friction velocity $u_\tau = \sqrt{\nu dU/dz}|_{z=0}$ is based on the kinematic viscosity ν and wall shear, free stream velocity (U_∞) is 20 m/s and boundary layer thickness (δ) is 0.35mm. The database for axisymmetric jets

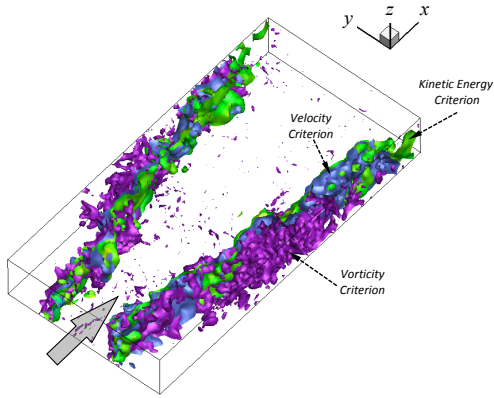


Figure 2: Three different interface detection criteria for applied to the volumetric data set of tomo-PIV.

is from the planar PIV and the tomographic-PIV measurements of [10] and [11]. An example from planar PIV of jet is shown in figure 1(b), where the jet diameter $d = 2\text{mm}$ and Reynolds number $Re_d \approx 3000$ (based on the inlet velocity, $U_o = 23\text{m/s}$, d and air as the working medium).

Figure 2 shows the jet interfaces based on three different detection criteria[1]: velocity criterion, $\tilde{U}/U_o = 0.03$ (in violet colour and the region with value > 0.03 is turbulent); vorticity criterion, $|\omega|r_{1/2}/U_c = 0.17$ (in blue colour, where, $|\omega|$ is the total vorticity magnitude, $r_{1/2}$ is the radial location where the centre line velocity U_c is $1/2$, and values > 0.17 is termed turbulent); and kinetic energy (KE) criterion, $|\mathbf{U}|^2/U_o^2 = 0.003$ (shown in green colour, where, $|\mathbf{U}|$ is the total velocity magnitude and values > 0.003 considered turbulent). Here, we utilise the KE criteria following [2] and [15], who provide a detailed discussion of the criteria for TNTI detection. The interfaces identified by the KE threshold are also shown in figures 1(a) and (b).

Using large-scale vortex rod calculations Philip *et.al* [14] has shown that there is a radial inflow into the turbulent region, whereas no such inflow exists in the case of wakes. It is well known that similar to wakes, there is no radial inflow in boundary layers (in fact the mean wall-normal velocity is towards the non-turbulent region in BLs) [18]. The radial inflow velocity is a major difference between jet and BL (as well as wake) entrainment.

To illustrate the radial velocity in jets, figure 3 shows an instantaneous TNTI (where the mean flow is in x -direction) along with velocity vectors on a plane in the irrotational region. It is evident that on this plane the flow is towards TNTI. Consequently radial inflow cannot be ignored while studying entrainment in jets, which is virtually non-existent in wakes and boundary layers. To further support this point, figure 4 shows the advection terms in the KE balance of the axisymmetric jet from tomo-PIV measurements, namely, the radial advection term $-0.5(U_r \partial \langle |\mathbf{u}|^2 \rangle / \partial r)$, the axial advection terms $-0.5(U_x \partial \langle |\mathbf{u}|^2 \rangle / \partial x)$, and the their sum, where, $|\mathbf{u}|$ is the magnitude of the fluctuating velocity vector. It is clear that even though the radial component is negligible towards the centre of the jet, it makes a significant contribution at the edge of the turbulent region (c.f., inset of figure 4). Furthermore, close to the boundary the radial advection is counter-balanced by turbulent diffusion (not shown here)[17].

Instantaneous velocity measurements (\tilde{U} - streamwise and \tilde{W} - wall-normal/radial) conditioned at the TNTI ($\langle \tilde{U} \rangle$ and $\langle \tilde{W} \rangle$, respectively) are more suitable to quantify the effects of the radial velocity. Figure 5 shows the conditional streamwise (top) and radial (bottom) velocities across the TNTI for the jet. Equivalent profile for the boundary layer is shown in figure 6. Note that

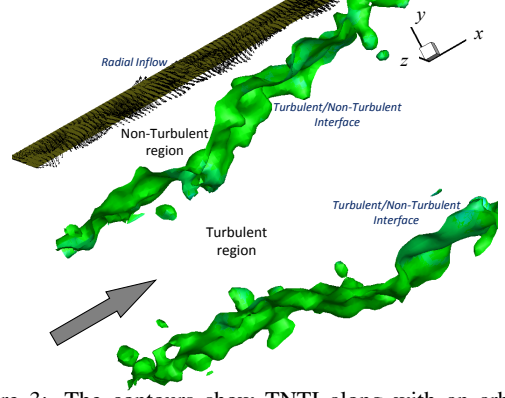


Figure 3: The contours show TNTI along with an arbitrary plane along the axial direction in the non-turbulent region and velocity vectors over that plane. The radial incoming flow through the plane is evident, and contributes to the overall entrainment.

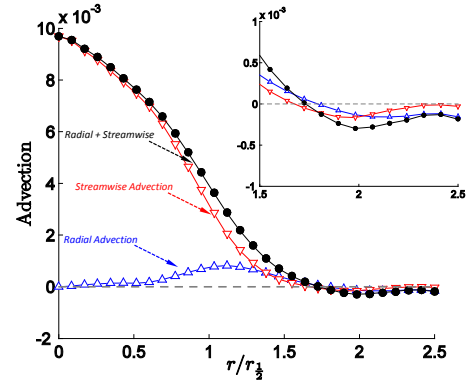


Figure 4: The advection terms from the KE balance. Inset shows the expanded view of the edge of the jet where the radial advection dominates the axial one, unlike in the core.

z_i is the wall-normal or the radial location of the TNTI. For the streamwise velocity both the jet and the BL shows the expected jump in velocity ($\Delta \tilde{U}$); however, normal velocities show rather distinct features. In the case of jets, in the non-turbulent region $\langle \tilde{W} \rangle$ becomes approximately equal to the radial velocity, unlike in BLs where $\langle \tilde{W} \rangle$ must approach zero in the far field [3]. Consequently, for jets (c.f bottom figure 5) we represent the peak velocity in the NT region as a sum of the radial velocity and an eddy/engulfment velocity (denoted by $\Delta \tilde{U}_{r(eddy)}$), whereas for BLs (c.f bottom figure 6) there is only eddy/engulfment velocity (denoted by $\Delta \tilde{W}_{(eddy)}$). It is recalled that the radial velocity is non-existent in BL flows.

Interestingly, the ratio $\Delta \tilde{W}_{(eddy)}/\Delta \tilde{U}$ for BLs is ≈ 0.1 , which is the same as the asymptotic value reported in [3] using a range of Re_τ in BLs. A similar ratio for the present jet is, $\Delta \tilde{U}_{r(eddy)}/\Delta \tilde{U} \approx 0.17$. Even though the jet measurements are only at one Re , the fact that the ratios in BL and jet is close, is rather suggestive of a similar (perhaps small-scale) mechanism that is present at the TNTI in both jets and BLs. A range of Re studies in jet flows is required to ascertain this. Consequently, it is suggested that if the radial velocity component from the jets is removed, the mechanism of entrainment in both jets and BLs could be similar. These distinguishing features motivate classification of the shear-flows into three different categories depending on the large- and small-scale entrainment features.

Classification of shear flows for entrainment

The premise here is that large-scales determine the rate of entrainment while the small-scale eddies residing on the interface of turbulent/non-turbulent region are responsible for the conver-

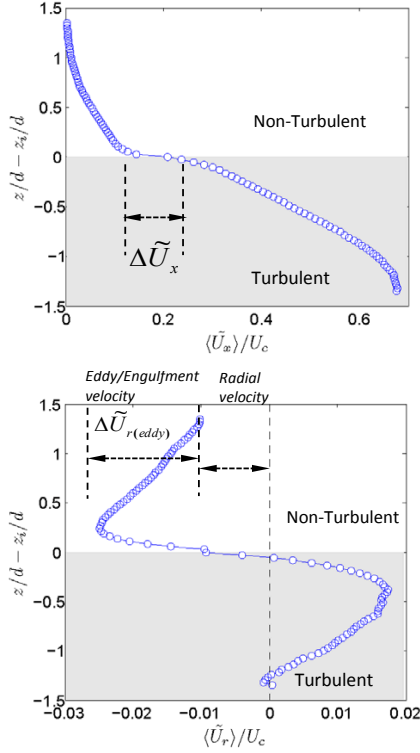


Figure 5: Conditional velocities at TNTI for a jet. Top: stream-wise, and bottom: radial velocities.

sion of the non-turbulent fluid into a turbulent state. It will be argued that large-scale or bulk motion is responsible for bringing the non-turbulent fluid close to the interface, whereas the small-scale ‘nibbling’ eddies at the interface act towards its the final conversion to turbulent fluid. Accordingly, we consider the large- and small-scale eddies as contributing towards a ‘multi-stage’ complimentary entrainment process, rather than a competing one.

The large-scale motions of the flow are envisaged to have three different roles in the entrainment process: L_1 - producing a net inflow towards the interface (such as in jets, where there is a mean radial inflow); L_2 - entrapment or ‘engulfment’ of the non-turbulent fluid; and L_3 - increasing the surface area of the interface by large-scale contortions. On the other hand, the small scales seem to play two roles: S_1 - the well accepted role of converting the NT fluid to turbulent one; and S_2 - ‘reaching out’ or ‘diffusing’ into the NT region. The challenge is to understand the relative importance of each of these processes in different flows.

As such, for the purpose of entrainment studies, shear flows are divided into three categories (also see, [14]): (1) where there is a bulk motion in the NT region towards the interface, such as in jets, where all processes L_1, L_2, L_3 and S_1, S_2 are likely; (2) where there is no bulk NT motion, such as, in wakes and boundary layers, where processes L_2, L_3 and S_1, S_2 are possibly active, and finally (3) where there is no large-scale motion, such as, in the oscillating-grid or shear-free flows (e.g., [8]), where only the processes S_1, S_2 are present.

Accordingly, figure 7 presents schematics of a jet on the top as panel 1, wakes and boundary layer flows as panel 2, and the oscillating grid or shear-free flow as panel 3, corresponding to the three categories. The large scale process of radial inflow (L_1) in jets is schematically shown in panel 1, whereas eddying motion (L_2) is present in both 1 and 2. The small-scale processes act in all the cases, however, shear-free flows have exclusively small-scale processes. Also shown are the order of magnitude

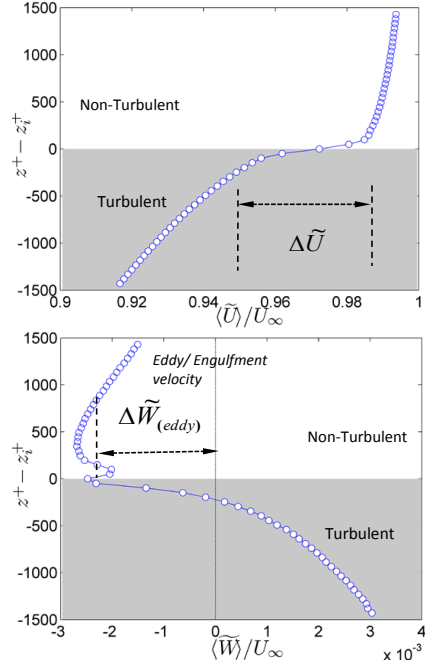


Figure 6: Conditional velocities at TNTI for a BL. Top: stream-wise, and bottom: wall-normal velocities.

of length scale of eddies, which are of order of large-scale, δ in shear flows, whereas it is of order of Taylor’s microscale, λ in the shear-free flows. The corresponding strain rates, say S , over a time scale of $1/S$, will produce length scale of order $\sqrt{\nu t}$ under the action of viscosity (where, ν is the kinematic viscosity and t , time). This implies that the interface thickness in shear flows are the order of λ and that in shear-free flows is η (where, η is the Kolmogorov length scale)[16, 4].

Spreading of shear flows

Both the ‘multi-stage’ [14] and ‘multi-scale’ [15] processes suggest that the final/smallest-scale process is governed by the local entrainment velocities. This motivates us to derive the overall large-scale growth of various shear flows from the scaling of the small-scale velocities. There are several valid methods which predict the spreading of free shear flows, such as jets and wakes, most of which rely on the equations of the conservation of overall momentum and/or energy (e.g., [18, 17]) with no recourse to small-scale motions. We, however, follow a succinct approach due to Landau and Lifshitz [12] for turbulent wakes, which includes elements of diffusion and extended here for jet and boundary layers including the scaling of local velocities at the TNTI.

Consider an axisymmetric turbulent wake (c.f. figure 7, panel 2), where δ is proportional to the radial width of the turbulent region, x the axial direction, U the mean flow in x (here assumed to be a constant) and u the order of the velocity fluctuations near the interface. Considering the averaged streamlines,

$$\frac{d\delta}{dx} \sim \frac{u}{U}. \quad (1)$$

Since drag $\sim Uu\delta^2$ is constant, $Uu \sim \delta^{-2}$, which along with the above equation gives the standard result that $\delta \sim x^{1/3}$. For the case of turbulent jets since $u \sim U$, the equation (1) again gives the standard result, $\delta \sim x$. In the case of turbulent boundary layers, the relevant fluctuating velocity scale at TNTI is u_τ . Now, if we use any empirical relation for the variation of u_τ with the streamwise distance x , say, the 1/7 law ($C_f \sim Re_x^{-1/7}$), $u_\tau^2 \sim x^{-1/7}$. Thus, with $u \sim x^{-1/14}$ and U equal to the constant

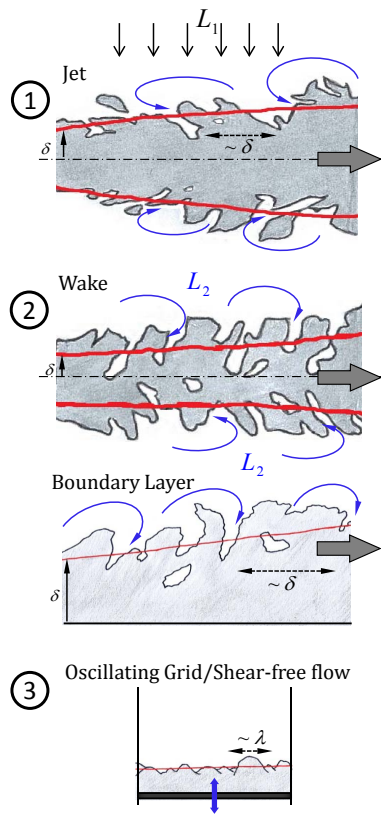


Figure 7: Classification of flows for the purpose of entrainment. Top figure, panel 1 : jet flow which exclusively includes the radial inflow process L_1 , as well as L_2 , L_3 , S_1 , and S_2 . Panel 2, wakes and boundary layers containing processes L_2 , L_3 , S_1 , and S_2 (refer main text for their definitions). Panel 3, oscillating-grid/shear-free flows, which has no large-scale processes but only small-scale ones S_1 and S_2 .

free stream velocity, equation (1) shows that $\delta \sim x^{13/14}$, which is again close to the experimental observations.

The important quantity in equation (1) is u , which is the velocity scale around TNTI, and has been taken to be the fluctuating component in the above analysis, consistent with the recent experimental evidence. Furthermore, under the local approximation of turbulent production equal to dissipation (with the local velocity scale being u), it is evident that (e.g. [17]), indeed Taylor microscale λ is the relevant length scale at the interface. So we arrive at the same conclusion as in the previous section, however from a different point of view that links the spreading in shear flows with the smaller scales present at the interface.

Acknowledgements

The authors gratefully acknowledge support from the Australian Research Council.

References

[1] Anand, R., Boersma, B. J. and Agrawal, A., Detection of turbulent/non-turbulent interface for an axisymmetric turbulent jet: evaluation of known criteria and proposal of a new criterion, *Exp. Fluids*, **47**, 2009, 995–1007.
 [2] Chauhan, K., Philip, J., de Silva, C., Hutchins, N. and Marusic, I., The turbulent/non-turbulent interface and entrainment in a boundary layer, *J. Fluid Mech.*, **742**, 2014, 119–151.

[3] Chauhan, K., Philip, J. and Marusic, I., Scaling of the turbulent/non-turbulent interface in boundary layers, *J. Fluid Mech.*, **751**, 2014, 298–328.
 [4] da Silva, C. B. and dos Reis, R. J. N., The role of coherent vortices near the turbulent/non-turbulent interface in a planar jet, *Phil. Trans. Royal Soc. Lond. A Math. Phys. Sci.*, **369**, 2011, 738–753.
 [5] da Silva, C. B., Hunt, J. C. R., Eames, I. and Westerweel, J., Interfacial layers between regions of different turbulence intensity, *Ann. Rev. Fluid Mech.*, **46**, 2014, 567–590.
 [6] da Silva, C. B. and Pereira, J. C. F., Invariants of the velocity-gradient, rate-of-strain, and rate-of-rotation tensors across the turbulent/nonturbulent interface in jets, *Phys. Fluids*, **20**, 2008, 055101.
 [7] de Silva, C. M., Philip, J., Chauhan, K., Meneveau, C. and Marusic, I., Multiscale geometry and scaling of the turbulent-nonturbulent interface in high Reynolds number boundary layers, *Phys. Rev. Lett.*, **111**, 2013, 044501.
 [8] Holzner, M., Liberzon, A., Nikitin, N., Kinzelbach, W. and Tsinober, A., Small-scale aspects of flows in proximity of the turbulent/nonturbulent interface, *Phys. Fluids*, **19**, 2007, 071702.
 [9] Holzner, M., Lüthi, B., Tsinober, A. and Kinzelbach, W., Acceleration, pressure and related quantities in the proximity of the turbulent/nonturbulent interface, *J. Fluid. Mech.*, **639**, 2009, 153–165.
 [10] Khashehchi, M., *Tomo-PIV Assessment of a Turbulent Round Jet*, Ph.D. thesis, The University of Melbourne, 2012.
 [11] Khashehchi, M., Ooi, A., Soria, J. and Marusic, I., Evolution of the turbulent/non-turbulent interface of an axisymmetric turbulent jet, *Exp. Fluids*, **54**, 2013, 1–12.
 [12] Landau, L. D. and Lifshitz, E. M., *Fluid Mechanics*, Pergamon Press, 1987.
 [13] Mathew, J. and Basu, A. J., Some characteristics of entrainment at a cylindrical turbulence boundary, *Phys. Fluids*, **14**, 2002, 2065–2072.
 [14] Philip, J. and Marusic, I., Large-scale eddies and their role in entrainment in turbulent jets and wakes, *Phys. Fluids*, **24**, 2012, 055108.
 [15] Philip, J., Meneveau, C., de Silva, C. M. and Marusic, I., Multiscale analysis of fluxes at the turbulent/non-turbulent interface in high Reynolds number boundary layers, *Phys. Fluids*, **26**, 2014, 015105.
 [16] Sreenivasan, K. R., Ramshankar, R. and Meneveau, C., Mixing, entrainment and fractal dimensions of surfaces in turbulent flows, *Phil. Trans. Royal Soc. Lond. A Math. Phys. Sci.*, **421**, 1989, 79–108.
 [17] Tennekes, H. and Lumley, J. L., *A first course in turbulence*, The MIT Press, 1972.
 [18] Townsend, A. A., *The structure of turbulent shear flow*, Cambridge University Press, 1976.
 [19] van Reeuwijk, M. and Holzner, M., The turbulence boundary of a temporal jet, *J. Fluid Mech.*, **739**, 2014, 254–275.
 [20] Westerweel, J., Fukushima, C., Pedersen, J. M. and Hunt, J. C. R., Mechanics of the turbulent-nonturbulent interface of a jet, *Phys. Rev. Lett.*, **95**, 2005, 174501.